DISCRETE AND CONTINUOUS
DYNAMICAL SYSTEMS SERIES B
Volume **16**, Number **1**, July **2011**

doi:10.3934/dcdsb.2011.16.57

pp. **57–71**

FINITE TO INFINITE STEADY STATE SOLUTIONS, BIFURCATIONS OF AN INTEGRO-DIFFERENTIAL EQUATION

Samir K. Bhowmik

Department of Mathematics, University of Dhaka
Dhaka 1000, Bangladesh

Dugald B. Duncan

Department of Mathematics and Maxwell Institute
Heriot–Watt University
Edinburgh, UK

Michael Grinfeld

Department of Mathematics, University of Strathclyde
Glasgow, UK

Gabriel J. Lord

Department of Mathematics and Maxwell Institute
Heriot–Watt University
Edinburgh, UK

(Communicated by Tim Healey)

Abstract. We consider a bistable integral equation which governs the stationary solutions of a convolution model of solid–solid phase transitions on a circle. We study the bifurcations of the set of the stationary solutions as the diffusion coefficient is increased to examine the transition from an uncountably infinite number of steady states to three for the continuum limit of the semi–discretised system. We show how the symmetry of the problem is responsible for the generation and stabilisation of equilibria and comment on the puzzling connection between continuity and stability that exists in this problem.

2000 *Mathematics Subject Classification.* Primary: 37G40; Secondary: 45K05.

Key words and phrases. Integro-differential equation, bifurcations, continuum limit, semi-discrete, regularity.

1. **Introduction.** Integro-differential equations are used to model phenomena in materials science [1, 2, 3, 5, 9, 18] and biology [7, 8, 21, 25] which involve non-local diffusion/dispersal mechanisms. We consider the integro-differential equation (IDE)

$$u_t = \varepsilon \left(\int_{\mathbb{R}} J^\infty(x-y)u(y,t)dy - u(x,t) \int_{\mathbb{R}} J^\infty(x-y)dy \right) + f(u), \tag{1}$$

where the $L^1(\mathbb{R})$ kernel J^∞ satisfies $J^\infty(x) \geq 0$, $J^\infty(x) = J^\infty(-x)$ and $f(u)$ is a bistable nonlinearity. Below we routinely consider $f(u) = u(1-u^2)$ and the kernel

$$J^\infty(x) = \sqrt{\frac{100}{\pi}} \exp(-100x^2), \tag{2}$$

so that $\int_{\mathbb{R}} J^\infty(x)\ dx = 1$. To obtain a well-defined problem, (1) has to be supplemented by an initial condition, $u(x,0) = u_0(x)$ from a suitable function space, see [16, 20, 17].

The convolution equation (1) is the L^2-gradient flow of the free energy functional

$$E(u) = \frac{1}{4}\varepsilon \int_{\mathbb{R}} \int_{\mathbb{R}} J^\infty(x-y) \left(u(y)-u(x)\right)^2 dxdy + \int_{\mathbb{R}} \hat{F}(u)dx, \tag{3}$$

where $\hat{F}(u,t)$ is the smooth double well potential, $\hat{F}'(u) = -f(u)$.

For an overview of the use of (1) in materials science, see [10]. There are many papers dealing with the mathematical analysis of this equation, which examine existence and stability of travelling waves [3], the structure of the stationary solutions set [2], propagation of discontinuities [11], coarsening [9] and long time behaviour [16, 20, 24, 12].

Note, in particular, that in [16] it is shown that if the diffusion coefficient ε is sufficiently large, a "Conway–Hopf–Smoller" type result holds: the only stable steady state solutions in $L^\infty(\mathbb{R})$ are the constant stable steady states of the kinetic equation $u_t = f(u)$. Thus, if we choose $f(u) = u(1-u^2)$, the stable states are $u = 1$ and $u = -1$. On the other hand, if $\varepsilon = 0$, (1) admits an uncountable set of equilibria. To see that, let X, Y and Z be any disjoint sets such that $X \cup Y \cup Z = \mathbb{R}$. Then a function $u(x)$ that is equal to 1 on X, -1 on Y and 0 on Z is a steady state solution. If $Z = \emptyset$, all the resulting equilibria are stable in $L^\infty(\mathbb{R})$. Furthermore, it is shown in [9] that there exists an $\varepsilon_0 > 0$ which depends on the kernel J^∞, such that for all $0 < \varepsilon < \varepsilon_0$ the set of steady state solutions of (1) is in one-to-one correspondence with the set of equilibria of $u_t = f(u)$. Hence, in view of the above, it is of interest to perform a bifurcation analysis of the set of steady states of (1),

$$0 = \varepsilon \int_{\mathbb{R}} J^\infty(x-y)(u(y)-u(x))\, dy + f(u), \tag{4}$$

as we decrease ε from some initially large value to zero, and investigate the transition from a finite to infinite set of solutions.

To the best of our knowledge, such a study has not been performed before. The object of this paper is precisely such a study of the spatially discretised version of (1). For simplicity, here we restrict ourselves to 1-periodic patterns.

If we choose spatially one-periodic initial data $u(x,0)$, from (1) it is clear that for all $x \in \mathbb{R}$ and $t \in \mathbb{R}_+$

$$u(x,t) = u(x+1,t).$$

Then from (1) we have

$$\begin{aligned} u_t &= \varepsilon \int_{\mathbb{R}} J^\infty(x-y)\,(u(y,t)-u(x,t))\,dy + f(u) \\ &= \varepsilon \sum_{r=-\infty}^{\infty} \int_r^{r+1} J^\infty(x-y)\,(u(y,t)-u(x,t))\,dy + f(u) \\ &= \varepsilon \sum_{r=-\infty}^{\infty} \int_0^1 J^\infty(x-z-r)\,(u(z+r,t)-u(x,t))\,dz + f(u) \\ &= \varepsilon \int_0^1 J(x-z)\,(u(z,t)-u(x,t))\,dz + f(u), \end{aligned} \tag{5}$$

where

$$J(x) = \sum_{r=-\infty}^{\infty} J^\infty(x-r) \tag{6}$$

and $x \in [0,1]$. Thus, for 1-periodic initial data we only need to solve the problem (1) on the interval $\Omega = [0,1]$ with the kernel $J(x)$. For the kernel given by (2), $J^\infty(x)$ and $J(x)$ are plotted in Figure 1.

Lemma 1.1. *For J defined by (6) the following two properties hold.*

1. *If $J^\infty(x) = J^\infty(-x)$ we have that $J(x) = J(-x)$ and*

$$J(x) = J(1-x).$$

2. $\int_0^1 J(x)\,dx = \int_{-\infty}^{\infty} J^\infty(x)\,dx$.

Property 1. above has an important influence on the spectrum of the matrix governing the semi-discretised version of (1) as we explain in the next section. From now on we work on $[0,1]$ and use the kernel J given in (6).

2. **The semi-discretised system.** We discretise in space using piecewise-constant functions [9] and collocating at the uniformly spaced element mid-points, $x = x_{j-\frac{1}{2}}$, $j = 1, 2, \cdots, N$. Setting $u_j = u(x_{j-\frac{1}{2}}, t)$, we have the semi-discrete approximation of (1) given by

$$u_t = \varepsilon A_N u + F(u), \tag{7}$$

where now $u(t) \in \mathbb{R}^N$, supplemented with some initial condition $u(0) \in \mathbb{R}^N$. The nonlinearity $F : \mathbb{R}^N \mapsto \mathbb{R}^N$ is given by $F_j(u) = f(u_j)$. It remains to specify the $N \times N$ matrix A_N. If we put $h = \frac{1}{N}$, and define $x_j = h(j - \frac{1}{2})$, $u_j = u(x_j, t) \in \mathbb{R}$, the elements of A_N are given by

$$a_{j,i} = \begin{cases} hJ\,(h|j-i|) & j \neq i \\ -h\left[\sum_{r=1, r\neq j}^{N} J\,(h|j-r|)\right] & j = i, \end{cases} \tag{8}$$

for all $i, j = 1, 2, \cdots, N$. From Lemma 1.1 it follows that A_N is a symmetric circulant matrix generated by the elements $a_{1,1}, \ldots, a_{1,N}$. Hence the theory of circulant matrices can be used to characterise its spectrum precisely. Let W_k be the N distinct roots of $z^N - 1 = 0$, so $W_k = \exp\left(\frac{i2\pi k}{N}\right)$, for $k = 0, 1, 2, ..., N-1$. Then the following theorem holds:

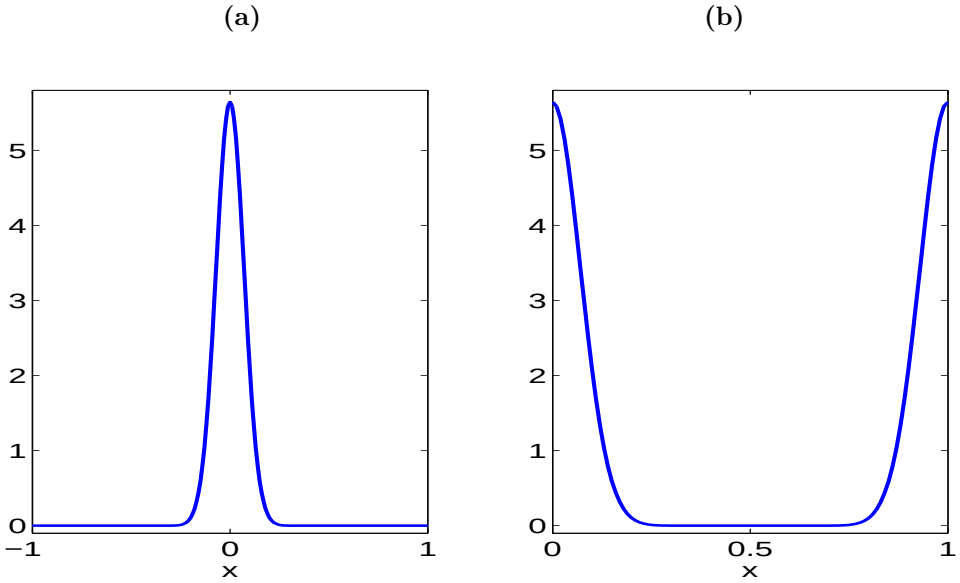

FIGURE 1. The kernels $J^\infty(x)$ in (a) and $J(x)$ in (b) for the case of equation (2).

Theorem 2.1 ([23])**.** *Let A_N be the circulant matrix defined by $a_{1,1}, a_{1,2}, ..., a_{1,N}$. Then $-A_N$ is diagonalisable with eigenvalues*

$$\lambda_k = -[a_{1,1} + a_{1,2}W_k + a_{1,3}W_k^2 + ... + a_{1,N}W_k^{N-1}], \tag{9}$$

with corresponding eigenvectors $v_k = \left(1, W_k, W_k^2, ..., W_k^{N-1}\right)^T$.

Let us see what this implies in our case for the spectrum of the discretisation.

Lemma 2.2. *The following three properties hold for the spectrum of A_N*

1. *$\lambda_0 = 0$;*
2. *$\lambda_k \in \mathbb{R}$ and $\lambda_k = \lambda_{N-k}$, $k = 1, 2, \cdots, N-1$;*
3. *As $N \to \infty$,*

$$\lambda_k \to \int_0^1 J(x)\,dx - \int_0^1 J(x)\exp(2\pi ikx)\,dx,$$

$k = 1, 2, \ldots$.

Before we prove this lemma, let us explain what it means. First of all, we must have a zero eigenvalue with a constant eigenvector, because, like in the case of the Neumann Laplacian, the equation

$$u_t = \int_{-\infty}^{\infty} J^\infty(x-y)(u(y,t) - u(x,t))\ dx,$$

conserves mass.

Secondly, the pairing of the eigenvalues is simply the consequence of the symmetry $J(x) = J(1-x)$ inherited from the evenness of the kernel J^∞. Finally, the third part of the lemma implies that as $N \to \infty$, the spectrum accumulates at the

point $\int_0^1 J(x)\,dx$. Note that in the case of $J^\infty(x) = \sqrt{100/\pi}\,\exp(-100x^2)$, we explicitly have

$$I_\infty = [1 - \exp(-\pi^2/100), 1] = [0.094, 1].$$

Proof. 1. From (8), putting $W_0 = 1$, we immediately obtain from (9) that $\lambda_0 = 0$.

2. From part 1. of Lemma 1.1 it follows using (9) that for all $j = 2, \ldots, N$,

$$a_{1,j} = a_{1,N+2-j},$$

so that the matrix A_N is symmetric. Hence its eigenvalues λ_k are real. But then taking complex conjugates of $A_N v_k = \lambda_k v_k$, we get that $A_N \overline{v_k} = \lambda_k \overline{v_k}$, or in other words $A_N v_{N-k} = \lambda_k v_{N-k}$ and hence $\lambda_k = \lambda_{N-k}$.

3. Taking the limit as $N \to \infty$ in (9) we immediately obtain the result. The integral $\displaystyle\int_0^1 J(x)\exp(2\pi i k x)\,dx$ is real since J is symmetric.

Note that this result implies that in the limit $N \to \infty$ the (discrete) spectrum of the convolution is contained in the interval

$$I_\infty = \left[\int_0^1 J(x)dx - \int_0^1 J(x)\exp(2\pi i x)\,dx, \int_0^1 J(x)dx\right],$$

with $\displaystyle\int_0^1 J(x)\,dx$ being an accumulation point. □

Our aim is to examine bifurcations in this system. Below we perform a numerical path–following of solution branches. Some of these will, by symmetry, arise in pitchfork bifurcations from the trivial solution $u = 0$. Here we examine analytically the values of ε where such bifurcations may occur in the semi-discrete system and later we can compare to the numerically found values. Linearising around the zero solution, we have the eigenvalue problem

$$\varepsilon A_N v + f'(0)v = \mu v, \tag{10}$$

and hence bifurcations from the zero solution will only occur if $\mu = 0$, or in other words, if

$$-A_N v = \frac{f'(0)}{\varepsilon} v.$$

Thus, for the semi-discrete system (7) we can fully characterize the values of ε where bifurcations of the zero solution occur, namely

$$\varepsilon_k := \frac{f'(0)}{\lambda_k},\ k = 0, \ldots, N-1. \tag{11}$$

For example, for $N = 32$, $J^\infty(x) = \sqrt{\frac{100}{\pi}}\exp(-100x^2)$ and $f(u) = u(1-u^2)$, we have using (9), the results of Lemma 2.2 and the formula (11) that bifurcations from the zero solution are expected at the values of ε as in Table 1. Note that for this case of $N = 32$, the value of ε_1 agrees to 12 decimal points with the limiting value of ε_1, $1/(1 - \exp(-\pi^2/100))$ as $N \to \infty$, (see part 3 of Lemma 2.2).

Let us examine the eigenvectors of $-A_N$ in some more detail. Since both v_k and v_{N-k} are eigenvectors, we immediately have that $\mathrm{Re}\,(v_k)$ and $\mathrm{Im}\,(v_k)$ are eigenvectors. Define the cyclic shift σ on $u = (u_1, \ldots, u_N) \in \mathbb{R}^N$ by

$$\sigma(u) = (u_N, u_1, \ldots, u_{N-1}),$$

then we have

$\varepsilon_1 = \varepsilon_{31}$	10.6403416996149		$\varepsilon_9 = \varepsilon_{23}$	1.00033746722800
$\varepsilon_2 = \varepsilon_{30}$	3.06584313146254		$\varepsilon_{10} = \varepsilon_{22}$	1.00005172586163
$\varepsilon_3 = \varepsilon_{29}$	1.69885748860222		$\varepsilon_{11} = \varepsilon_{21}$	1.00000650971543
$\varepsilon_4 = \varepsilon_{28}$	1.25968856776757		$\varepsilon_{12} = \varepsilon_{20}$	1.00000067252291
$\varepsilon_5 = \varepsilon_{27}$	1.09266327932320		$\varepsilon_{13} = \varepsilon_{19}$	1.00000005703325
$\varepsilon_6 = \varepsilon_{26}$	1.02948119722480		$\varepsilon_{14} = \varepsilon_{18}$	1.00000000397031
$\varepsilon_7 = \varepsilon_{25}$	1.00800141737791		$\varepsilon_{15} = \varepsilon_{17}$	1.00000000022729
$\varepsilon_8 = \varepsilon_{24}$	1.00180943793728		ε_{16}	1.00000000002128

TABLE 1. For $N = 32$ Bifurcation values in terms of ε of the zero solution.

Lemma 2.3. *If v is a real eigenvector of $-A_N$ corresponding to a double eigenvalue λ, then so is $\sigma(v)$.*

This follows since if v is an eigenvector, then so is $e^{2i\pi/N}v$.

Remark. In the above argument, we can pass to the limit as $N \to \infty$ and conclude that $\cos(2\pi kx)$ and all their translates are eigenfunctions of $-A = -(\int_0^1 J(x-y)(u(y)-u(x))\,dy)$ no matter what the kernel $J(x)$ is as long as it has the right symmetry property. Of course, cosines are also the eigenfunctions of the Neumann Laplacian.

Finally we note that fixed points of the semi-discrete problem satisfy

$$0 = \varepsilon A_N u + F(u). \tag{12}$$

Thus at $\varepsilon = 0$ stable solutions are given by

$$u = \begin{cases} 1 & x \in X, \\ -1 & x \in Y \end{cases} \tag{13}$$

where $X \cup Y = [0,1]$. Unstable solutions at $\varepsilon = 0$ are given by

$$u = \begin{cases} 1 & x \in X, \\ -1 & x \in Y, \\ 0 & x \in Z \end{cases} \tag{14}$$

where $X \cup Y \cup Z = [0,1]$ with some nonempty Z.

We can now define solutions with different numbers of interfaces. When $X = [0,\alpha)$ and $Y = [\alpha,1]$, $0 < \alpha < 1$, we call u a *one-interface* solution of (12) if for $\varepsilon = 0$ for some $n \in [0, N-1]$, $\sigma^n(u) = a_1$ on $X = [0,\alpha)$ and $\sigma^n(u) = a_2$ on $Y = [\alpha,1]$, where a_1, $a_2 \in \{-1,0,1\}$ and $a_1 \neq a_2$. That is, we have at $\varepsilon = 0$ one jump in the solution up to a cyclic shift. Two-interface, three-interface solutions, etc., are defined similarly. We call a function with m discontinuities in $[0,1)$ a $m-1$ interface solution. Thus, for example, the branch of solutions corresponding to orbit A in Table 2 are of one-interface and those corresponding to E are of three-interface.

3. Results.

We take for our computations the kernel function

$$J^\infty(x) = \sqrt{\frac{100}{\pi}} e^{-100x^2},$$

with $f(u) = u(1-u^2)$ and vary the parameter ε. For small values of N it is possible to enumerate all possible solutions of the semi-discrete system (12) with $\varepsilon = 0$

and to analyse their continuation to $\varepsilon > 0$ using the theory of bifurcation with symmetry. This we do below for $N = 4$ and these analytic results are used to check the validity of our numerics.

We implement in MATLAB a standard pseudo arc–length continuation algorithm with step size control as described in [15, 22, 14] for the discrete problem (12). Since A_N is a circulant matrix, we take advantage of reducing storage costs as the full information of A_N can be obtained storing one row or column only, see [4] and references therein. Furthermore the use of the FFT for each matrix vector multiplication reduces the computational cost. We detect bifurcation points by observing where eigenvalues of the Jacobian $\mathcal{J} = D_u F$ of the nonlinear system $F(u, \beta) = 0$ cross the imaginary axis and perform branch switching at those points by perturbing in the direction of the associated eigenvector.

The arc-length ℓ of $u(x) \in C^1(\Omega)$ is defined in the standard way

$$\ell = \int_\Omega \sqrt{1 + \left(\frac{du}{dx}\right)^2}\, dx.$$

We approximate the arc–length of $u(x)$ with the mid-point rule and using the standard forward difference approximation for the derivative. With a uniform discretisation we get

$$\ell \approx \ell_h = \sum_{j=1}^{N} \sqrt{h^2 + (u_{j+1} - u_j)^2} \tag{15}$$

where $h = x_{j+1} - x_j$ and $u_j = u(x_j)$. Note that although ℓ only makes sense for $u \in C^1$, we can evaluate ℓ_h even when u is discontinuous at grid points.

For $N = 32$ we compute the bifurcation diagram numerically and gain insight into the structure of the bifurcation diagram of the original continuous problem.

Finally, we examine the large N limit and formulate the results of the numerics as two conjectures concerning the interplay of continuity and stability and the behaviour of saddle-node bifurcations as $\alpha \to 1/2$.

3.1. **The $N = 4$ case.** For the continuous system, the symmetry group is $O(2)\times\mathbb{Z}_2$, and so for a finite number of nodes N, we use $\Gamma_N = D_N \times \mathbb{Z}_2$ equivariance structure [13, 19].

If $N = 4$, there are 81 possible steady states at $\varepsilon = 0$, 16 of them stable. The group Γ_4 is generated by the shift p, the flip f and the reversal m. In terms of $v = (v_1, v_2, v_3, v_4)$, we have that

$$p(v) = (v_2, v_3, v_4, v_1);$$

$$f(v) = (v_4, v_3, v_2, v_1);$$

$$m(v) = (-v_1, -v_2, -v_3, -v_4);$$

Inverses of the nonzero eigenvalues of the 4×4 matrix A_4 are $\{91.82, 183.63, 183.63\}$, so we expect primary branches to bifurcate from the zero solution at those values of ε. Note that all primary branches have zero mean, but the converse is not true.

Since here we know all the solutions at $\varepsilon = 0$ and their stability, and since symmetry properties are conserved on primary branches, we can cut down the work considerably by looking only at orbits of solutions under Γ_4. In Table 2, we collect

Name	Orbit	length	Σ_x	Name	Orbit	length	Σ_x
	(0,0,0,0)	1	$D_4 \times \mathbb{Z}_2$	E	(-1,1,-1,1)	2	$\langle pm, fp \rangle$
	(1,1,1,1)	2	D_4	F	(0,1,0,0)	8	$\langle fp \rangle$
A	(-1,1,1,-1)	4	$\langle f, p^2 m \rangle$	G	(1,0,0,-1)	8	$\langle mf \rangle$
B	(1,0,-1,0)	4	$\langle mp^2, fp \rangle$	H	(0,1,0,1)	4	$\langle p^2, fp \rangle$
C	(0,0,1,1)	8	$\langle f \rangle$	I	(0,1,-1,1)	8	$\langle fp \rangle$
D	(0,-1,1,1)	16	$\langle I \rangle$				
				J	(0,1,1,1)	8	$\langle fp \rangle$
				K	(-1,1,1,1)	8	$\langle fp \rangle$

TABLE 2. Steady states for $N = 4$, the length of the orbits and isotropy subgroups Σ_x. We have separated the solutions into the homogeneous states, those connected with the first and second bifurcation of $u = 0$ and the two solutions connected by a saddle-node J and K. See also Figure 2.

all the orbits, their lengths and the corresponding isotropy subgroups Σ_x. There, $\langle f \rangle$ stands for the group generated by $f \in D_4 \times \mathbb{Z}_2$, etc.

Now we can immediately draw the bifurcation diagram using the following three rules [13, 19]:

1. A bifurcating branch must have the isotropy subgroup which is a subgroup of the isotropy group of the primary branch.

2. Dimensions of unstable manifolds have to match at a bifurcation point (to satisfy the principle of exchange of stability) and at $\varepsilon = 0$.

3. The number of nodal domains must increase from one bifurcation point to the next.

With these rules there is only one way to construct the bifurcation diagram; see Figure 2 (a) and (b), where the y-axis is not to any scale, and is only intended to make clear the end-points of various branches at $\varepsilon = 0$. These figures show the bifurcation structure arising from bifurcations of the zero solution.

We would like to make the following observations. The stable non-zero-mean branches corresponding to the orbit K have to arise through a saddle-node bifurcation. Numerically, this happens at a value of $\varepsilon \approx 49.294$ that is smaller than the value $\varepsilon_4 = 122.432$ at which the branches of the orbit A become stable; see Figure 3 which shows the equivalent numerically computed diagram. We will see the equivalents of these statements in higher dimensional discretisations. Note that in the numerics in Figure 3 the branches F and G have bifurcations at nearby values of ε ($\varepsilon \approx 73.452$ and $\varepsilon \approx 73.526$) and the two separate bifurcations can not easily be distinguished.

We did not perform a Liapunov–Schmidt calculation to determine the order of bifurcations at the double eigenvalue point $\varepsilon = 183.63$, but any assignment of stabilities different from that of Figure 2 cannot be reconciled with the above rules of bifurcation.

3.2. **The case of $N = 32$.** Though an analysis similar to that in the case of $N = 4$ can be attempted here, the numbers of orbits are astronomical, and we rely on our numerical continuation method, the results of which match exactly the predictions of the analysis in the case $N = 4$. In Figure 4 we plot in (a)–(d) sample solution

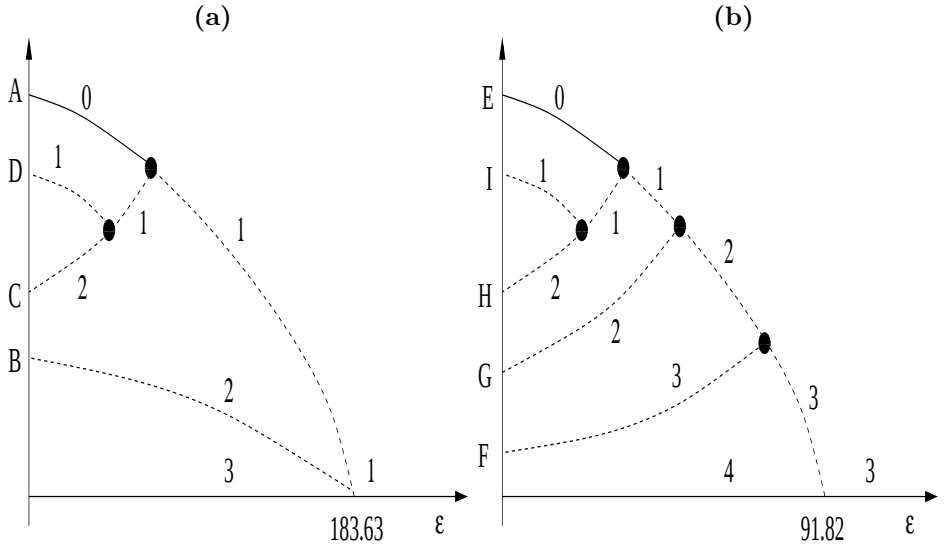

FIGURE 2. Bifurcations from the zero solution from the first (a) and second (b) bifurcation points. Solid lines represent stable and broken lines unstable solutions respectively. We indicate above each branch the dimension of the unstable manifold. We do not show the homogeneous solutions or the orbits J and K (which are connected by a saddle-node bifurcation).

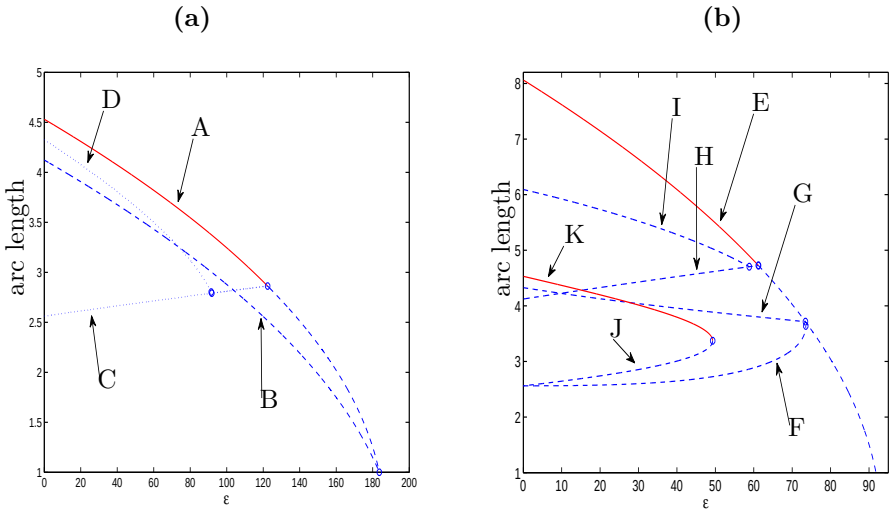

FIGURE 3. Numerically computed bifurcation diagram from the zero solution from the first (a) and second (b) bifurcation points. Solid lines represent stable and broken lines unstable solutions respectively We show the homogeneous solutions or the orbits J and K connected by a saddle-node bifurcation on (b). Compare to the theoretical prediction in Figure 2.

branches of the bifurcation diagram with $N = 32$. If we start with a large value of ε we see in (a) and (b) the first bifurcation arises at $\varepsilon \approx 10.64$ as predicted by the theory in Table 1. In (a) we show the continuation of the zero mean one-interface which undergoes a pitchfork bifurcation at $\epsilon \approx 2.012$. In (b) we have plotted the one-, three-, five- and seven- interface solutions and their stabilization. In (c) we show details of the bifurcation structure close to the pitchfork at $\varepsilon \approx 2.012$ (note for clarity one branch of the pitchfork seen in (a) is not plotted). As $\alpha \to 0.5$, the saddle-node bifurcation points converge to the value of where the zero mean one-interface which undergoes a pitchfork bifurcation at $\epsilon \approx 2.012$. This structure is repeated for the other n-interface solutions and is illustrated in (d) for the three-interfaces solutions. Here we see that the zero-mean one-interface solution branches stabilize at $\varepsilon \approx 2.012$. Below we will formulate a conjecture concerning the limiting value which we will call ε_1^s at which the one-interface branch with zero-mean stabilizes as $N \to \infty$.

4. **The limiting problem and conclusions.** It is not hard to prove (see for example [3]) that if $\varepsilon > 1$, steady state solutions of (4) are continuous, since the function $-\varepsilon u + f(u)$ is monotone. Hence it is interesting to understand when the solutions lose continuity (certainly, for $\varepsilon = 0$ there are no non-constant *continuous* solutions).

The non-trivial stable one-interface zero-mean solution branches ($\alpha = 0.5$) that originate at $\varepsilon = 0$ were investigated in detail as we change N. Define

$$M := \max_j \left| \frac{u_{j+1} - u_j}{h} \right|.$$

For a C^1 function this converges to $\max_{x\in[0,1]} |u_x|$ and so we can identify where the solution is continuous.

Figure 5 plots in (a) M against ε along a branch of one-interface zero-mean solutions for $N = 2^p$, $p = 4, 5, 6, 7, 8, 9, 10$. Let ε_m^d be the value of ε at which solutions on the zero-mean $2m-1$-interface branch become discontinuous. Then this figure suggests that $N \to \infty$, $\varepsilon_1^d \to 1$. This conclusion is supported in (b) which shows for different ε convergence of the derivative M with N on a log log scale.

Furthermore the loss of continuity appears to coincide with the gain of stability (equivalently the gain of continuity appears to coincide with the loss of stability). If ε_m^s is the value at which the zero-mean $2m-1$-interface solution becomes stable, in Figure 6 we show numerically that the bifurcation values converge to $\varepsilon_1^s = \varepsilon_2^s = 1$ as $N \to \infty$.

Now we can collect our observations and form two conjectures. First we consider the zero-mean interface branches.

Conjecture 1: $\varepsilon_m^s = \varepsilon_m^d$.

We can prove a very weak form of this conjecture for $m = 1$. From the results of [3] it follows that discontinuous stationary solutions will exist for any ε such that the function

$$g(u) := -\varepsilon u \int_0^1 J(s)\, ds + f(u)$$

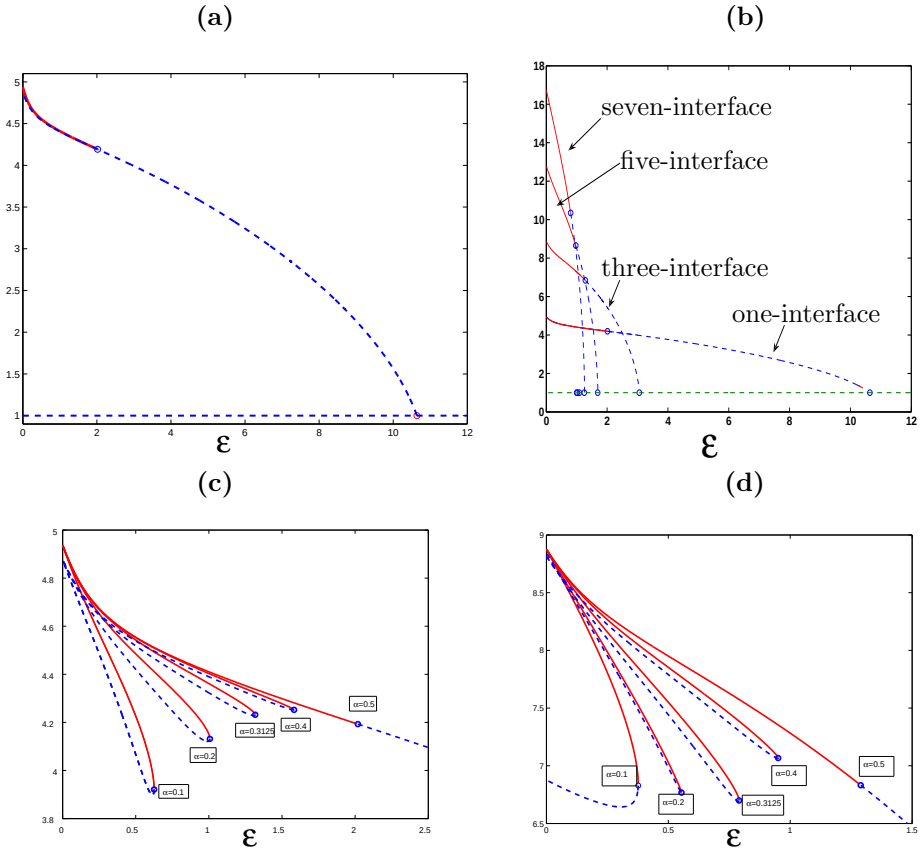

FIGURE 4. (a) Continuation of the zero-mean one-interface ($\alpha = 0.5$) solution branch. When $\varepsilon \approx 2.012$ shown by 'o' there is a stabilizing pitchfork bifurcation. (b) Stabilization of one-, three-, five-, and seven-interface solutions. (c) This is a blow up of the bifurcation diagram around the stabilizing bifurcation at $\varepsilon \approx 2.012$ shown by 'o' for the $\alpha = 0.5$ curve. Here stable solutions are continued from $\varepsilon = 0$ with different ratios (α) of -1 and 1 values of α. (d) A similar structure is observed starting from $\varepsilon = 0$ with two–interface solutions with different ratios (α) of -1 and 1. In (c) and (d) we examine $\alpha = 0.1$, $\alpha = 0.2$, $\alpha = 0.3125$, $\alpha = 0.4$ and $\alpha = 0.5$.

is non-monotone. On the other hand, from Theorem 2.1 of [6] it follows if $g(u)$ is monotone, there are no nonconstant minimizers of the energy functional (3). Hence we have $\varepsilon_1^s \leq \varepsilon_1^d$.

We now consider the saddle-node bifurcation of the non–zero mean interface solutions. Now, let u_r be a branch of $2m-1$-interface stable solutions of (4) with mean r, and let $\varepsilon_m^{\mathrm{bif},r}$ be the value of ε at which the saddle-node bifurcation giving rise to the branch occurs. Then we have

Conjecture 2: $\lim_{r\to 0} \varepsilon_m^{\mathrm{bif},r} = \varepsilon_m^s$.

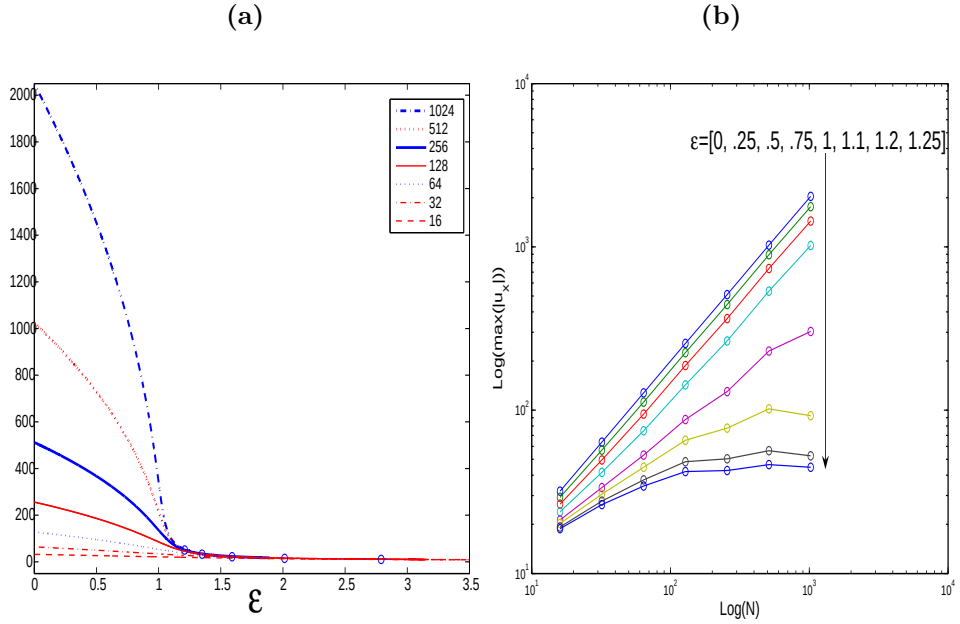

FIGURE 5. (a) The maximum of $|u_x|$ in $[0,1]$ of the solution $u(x)$ for one-interface initial data with ± 1 and $\alpha = 0.5$. (b) $\max_x(|u_x|)$ for different system sizes for particular values of ε with system size as the x-axis; note a clear change in behaviour at $\varepsilon = 1$.

These two conjectures, if true, would lead to the bifurcation picture sketched in Figure 7. In (a) we plot the zero-mean one-interface branch and have indicated the continuum of saddle–node bifurcations ε_1^s that approach the bifurcation at $\varepsilon_1^s = \varepsilon_1^d = 1$. In (b) we indicate the first four branches of the infinite number that bifurcate from zero, the branches of associated saddle-node bifurcations and here we have that $\lim_{r\to 0} \varepsilon_m^{\mathrm{bif},r} = \varepsilon_m^s = \varepsilon_m^d$. In addition our numerical investigation seems to indicate that $\varepsilon_1^s = \varepsilon_1^d = 1 = \varepsilon_2^s = \varepsilon_2^d$.

Finally, let us consider stable solutions, that is the solutions we expect to see from any simulation of dynamics. For $\varepsilon > 1$ we have two stable solutions, then a region of parameter space with an infinite number of stable solutions of one- and three-interface type, then a region of parameter space with one, three and five interfaces and so on. In conclusion the diffusion coefficient ε determines the number and type of stable solutions - from two to an infinite number for a finite value of ε unlike the classical Allen-Cahn equation.

REFERENCES

[1] P. Bates and F. Chen, *Periodic travelling waves for a nonlocal integro-differential model*, Electronic Journal of Differential Equations, **1999** (1999), 1–19.

[2] P. W. Bates and A. Chmaj, *A discrete convolution model for phase transitions*, Arch. Ration. Mech. Anal., **150** (1999), 281–305.

[3] P. W. Bates, P. C. Fife, X. Ren and X. Wang, *Travelling waves in a convolution model for phase transitions*, Archive for Rational Mechanics and Analysis, **138** (1997), 105–136.

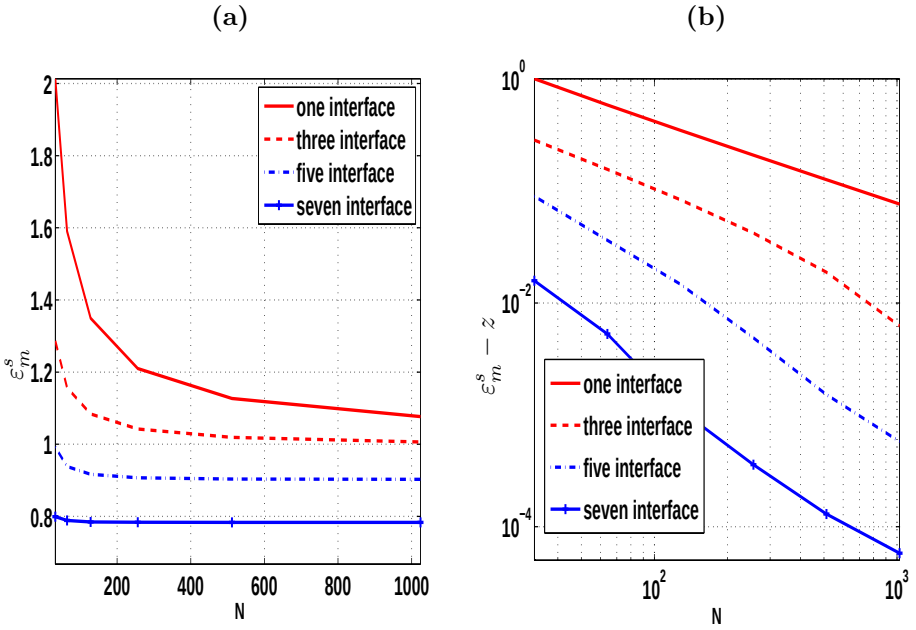

FIGURE 6. (a) Pitchfork bifurcations of the first $(2m-1)$–interface solutions as N increases. (b) A log-log plot of $\varepsilon - z$ versus N showing convergence to $z = 1, 1, 0.9, 0.7839$ for the one-, three-, five- and seven-interface solutions.

[4] S. K. Bhowmik, "Numerical Approximation of a Nonlinear Partial Integro-Differential Equation," PhD thesis, Heriot-Watt University, Edinburgh, UK, April, 2008.

[5] F. Chen, *Uniform stability of multidimensional travelling waves for the nonlocal Allen-Cahn equation*, Fifth Mississippi State Conference on Differential Equations and Computational Simulations, Electronic Journal of Differential Equations, Conference, **10** (2003), 109–113.

[6] A. Chmaj and X. Ren, *The nonlocal bistable equation: stationary solutions on a bounded interval*, Electr. J. Diff.eqns., **2002** (2002), 1–12.

[7] J. Coville and L. Dupaigne, *Propagation speed of travelling fronts in non local reaction-diffusion equations*, Nonlinear Analysis, **60** (2005), 797–819.

[8] K. Deng, *On a nonlocal reaction-diffusion population model*, DCDS series B., **9** (2008), 65–73.

[9] D. B. Duncan, M. Grinfeld and I. Stoleriu, *Coarsening in an integro-differential model of phase transitions*, Euro. Journal of Applied Mathematics, **11** (2000), 511–523.

[10] P. C. Fife, *Models of phase separation and their mathematics*, Electronic Journal of Differential Equations, **48** (2000), 1–26.

[11] P. C. Fife, *Well-posedness issues for models of phase transitions with weak interaction*, Nonlinearity, **14** (2001), 221–238.

[12] J. Garcia Melian and J. D. Rossi, *Logistic equation with refuge and nonlocal diffusion*, Communications on Pure and Applied Analysis, **8** (2009), 2037–2053.

[13] M. Golubitsky, I. N. Stewart and D. G. Schaeffer, "Singularities and Groups in Bifurcation Theory: Vol. **II**," Springer-Verlag, New York, 1988.

[14] W. J. F. Govaerts, *Numerical bifurcation analysis for ODEs*, Journal of Computational and Applied Mathematics, **125** (2000), 57–68.

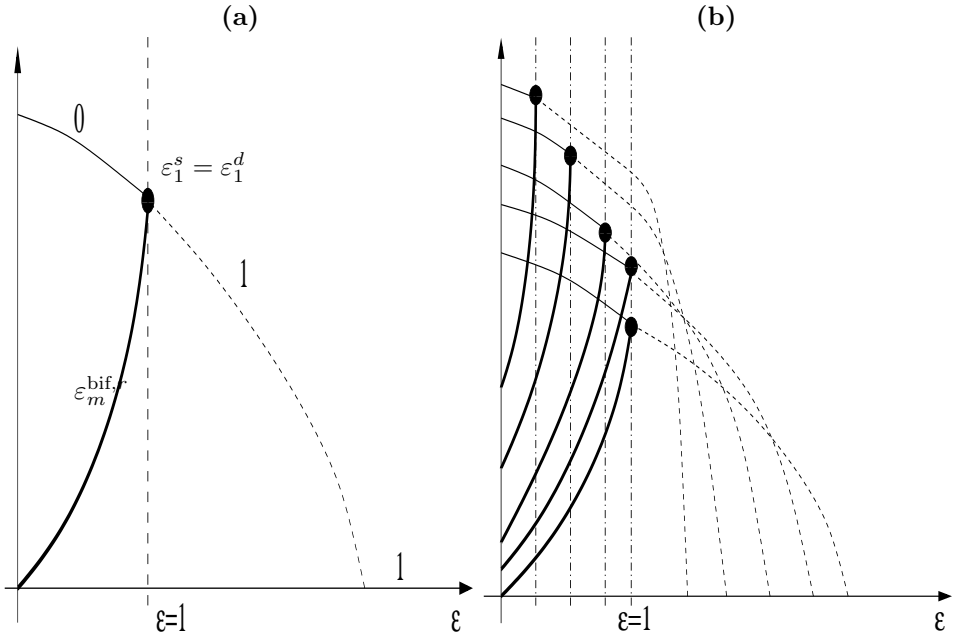

FIGURE 7. (a) Proposed bifurcation diagram for the one-interface solutions in the $N = \infty$ case. We show the primary branch and the continuum of saddle-node from the saddle–node bifurcations. In (b) we indicate that this structure is then repeated for the three-interface, five-interface,... solutions. The solid circles represent $\lim_{r\to 0} \varepsilon_m^{\mathrm{bif},r} = \varepsilon_m^s = \varepsilon_m^d$. The bifurcations for the one- and three-interface solutions both occur at $\varepsilon = 1$.

[15] W. J. F. Govaerts, "Numerical Methods for Bifurcations of Dynamical Equilibria," SIAM, Philadelphia, 2000.

[16] M. Grinfeld, W. Hines, V. Hutson, K. Mischaikow and G. Vickers, *Non-local dispersal*, Differential and Integral Equations, **11** (2005), 1299–1320.

[17] M. Grinfeld and I. Stoleriu, *Truncated gradient flows of the van der Waals free energy*, Electron. J. Diff. Eqns., **2006** (2006), 1–9.

[18] T. Hartley and T. Wanner, *A semi–implicit spectral method for stochastic nonlocal phase-field models*, DCDS, **25** (2009), 399–429.

[19] R. B. Hoyle, "Pattern Formation: An Introduction to Methods," Cambridge University Press, Cambridge, 2006.

[20] V. Hutson and M. Grinfeld, *Non-local dispersal and bistability*, Euro. Journal of Applied Mathematics, **17** (2006), 211–232.

[21] J. Medlock and M. Kot, *Spreading disease: Integro-differential equations old and new,* Mathematical Biosciences, **184** (2003), 201–222.

[22] Z. Mei, "Numerical Bifurcation Analysis for Reaction-Diffusion Equations," Springer, 2000.

[23] K. E. Morrison, *Spectral approximation of multiplication operators*, New York Journal of Mathematics, **1** (1995), 75–96.

[24] J. D. Rossi and A. F. Pazoto, *Asymptotic behaviour for a semilinear nonlocal equation*, Asymptotic Analysis, **52** (2007), 143–155.

[25] H. R. Wilson and J. D. Cowan, *Excitatory and inhibitory interactions in localized populations of model neurons*, Biophys. J, **12** (1972), 1–24.

Received April 2010; revised November 2010.

E-mail address: Bhowmiksk@gmail.com
E-mail address: D.B.Duncan@hw.ac.uk
E-mail address: M.Grinfeld@strath.ac.uk
E-mail address: G.J.Lord@hw.ac.uk